A lattice Boltzmann approach for three-dimensional tsunami simulation based on the PLIC-VOF method

Kenta Sato[1]   Shunichi Koshimura[2]

[1]Graduate School of Engineering, Tohoku University, Japan

[2]International Research Institute of Disaster Science, Tohoku University, Japan

2nd August, 2018

Background: Three-dimensional tsunami simulations

Conventional Free surface modelings

- Volume of fluid (VOF) method by FDM or FEM
- CIP advections based on Level-Set functions (Akkerman *et al.* 2011, Himeno *et al.* 2012, Balabel 2015)
- Lagrangian Meshfree methods by ISPH or MPS (Asai *et al.* 2012, Sarfaraz & Pak 2017, Hori *et al.* 2018)

The problem of the three-dimensional fluid simulations

Solving Navier-Stokes equation?

$$\frac{\partial \boldsymbol{u}}{\partial t} + (\boldsymbol{u} \cdot \nabla)\, \boldsymbol{u} = -\frac{1}{\rho}\nabla p + \nu \nabla^2 \boldsymbol{u} + \boldsymbol{g}$$

→ Very high-cost to determine pressure

Setup LBM: The lattice Boltzmann Method

An alternative to standard solver

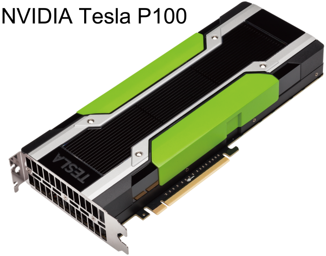

The key features of LBM

- Explicit in time stepping
- Highly parallelizable (local data)

The purpose of our research

Development of a three-dimensional high-performance tsunami simulation model

Setup LBM: What is the LBM?

An alternative numerical simulation method

- A mediator between macro-scale and micro-scale
  → A meso-scale analysis method (i.e. statistical method)
- Second-order accuracy in spacing discretization

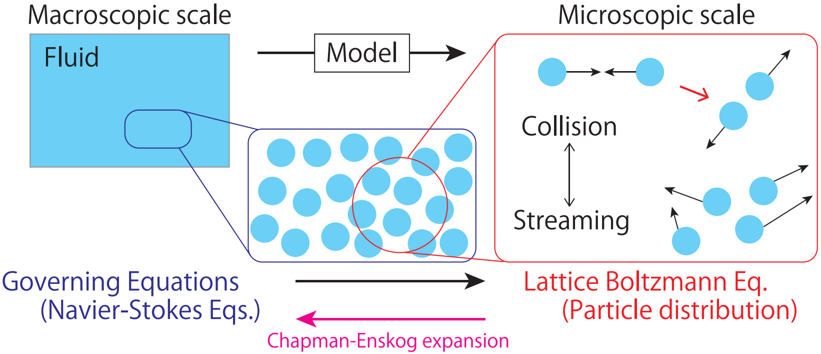

Figure: A schematic illustration of the LBM's basic concept

Setup LBM: How to model flows

Fluid dynamics modeling

- Fluid movements are altered as virtual particles' movements
- Solving the distributions by the simple linear equation
- In 3D model: 19 distribution functions (DFs) per grid

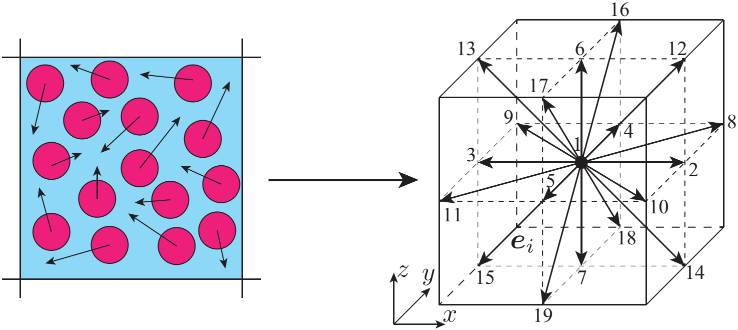

Figure: The three-dimensional nineteen-speed (D3Q19) lattice model

Setup LBM: The basic algorithm of LBM

The lattice Boltzmann equation (the Lattice BGK equation)

$$\underset{\text{Streaming}}{\underline{f_\alpha\left(\boldsymbol{x}+\boldsymbol{e}_\alpha \Delta t, t+\Delta t\right)-f_\alpha\left(\boldsymbol{x}, t\right)}}=\underset{\text{Collision}}{\underline{-\frac{1}{\tau}\left[f_\alpha\left(\boldsymbol{x}, t\right)-f_\alpha^{eq}\left(\rho, \boldsymbol{u}\right)\right]}}$$

f_α^{eq} → The equilibrium distribution functions, kernel function

$$f_\alpha^{eq}=w_\alpha\left[\rho+3 e_\alpha \boldsymbol{u}+\frac{9}{2}\left(\boldsymbol{e}_\alpha \boldsymbol{u}\right)^2-\frac{3}{2} \boldsymbol{u} \cdot \boldsymbol{u}\right]$$

where, ρ: macroscopic fluid density, $\boldsymbol{u}$: velocities

- For all grids:
  1. Streaming: the functions move to the neighboring cells
  2. Collision: the functions collide by BGK model, purely local

LBM's free surface model

The Volume of Fluid (VOF) approach (Thürey 2007)

- Advantages
  1. Free surface movements calculated by DFs
  2. Easy to parallelize the program on GPU (Janßen *et al.* 2013)
- Defects
  1. Non-physical discontinuously interfaces
  2. The fluid mass (total fluid volume in simulation) loss

The main purpose of our research

Development of LBM's VOF model by PLIC

Free surface model based on the VOF method

Cells' status

- Fluid fraction C: Division cells into three types

$$Cell's\,Type = \begin{cases} Gas & (C = 0) \\ Fluid & (C = 1) \\ Interface & (Otherwise) \end{cases}$$

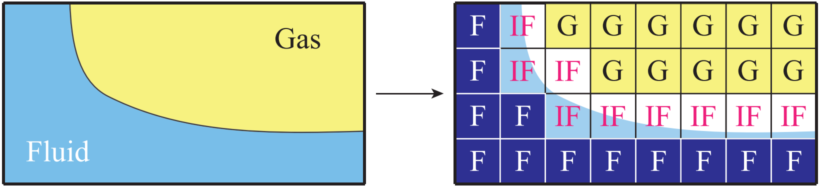

F	IF	G	G	G	G	G	G
F	IF	IF	G	G	G	G	G
F	F	IF	IF	IF	IF	IF	IF
F	F	F	F	F	F	F	F

Figure: The cell types required for the VOF method

Piecewise Linear Interface Reconstruction (PLIC-VOF)

More accurate interface modeling concept

Interface shapes

- SLIC-VOF → Rectangular shapes
- PLIC-VOF → Trapezoid shapes ($\boldsymbol{n} \cdot \boldsymbol{x} = \alpha$)

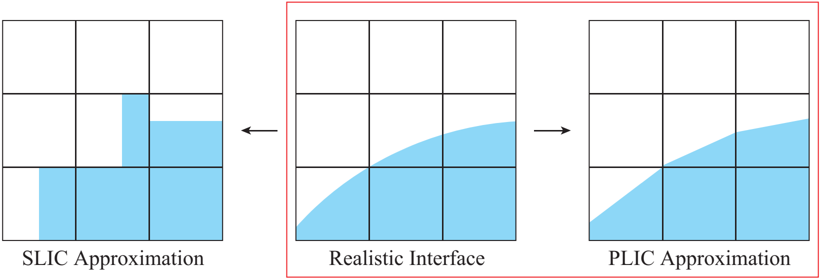

Figure: Interface reconstruction

Basic algorithm of the PLIC-VOF

1. determine the interface normal ($\boldsymbol{n} = -\nabla C / \|C\|$)
2. reconstruct interface (determine parameter α)
3. determine fluid flux and evaluate the new fill level C^{t+1}

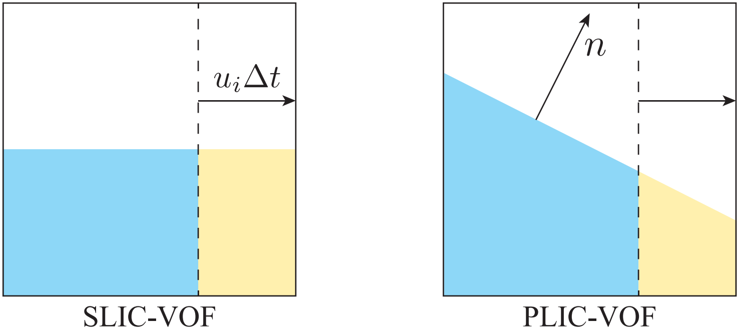

Figure: The advection of interfaces cells

V&V: Classical dam-breaking flows

A V&V of MRT-LBM's capability of handling realistic fluid

- Koshizuka *et al.* (2009), Martin & Moyce (1952)
- Verification: Spacing density profiles
- Validation: Dimensionless position of the surge front

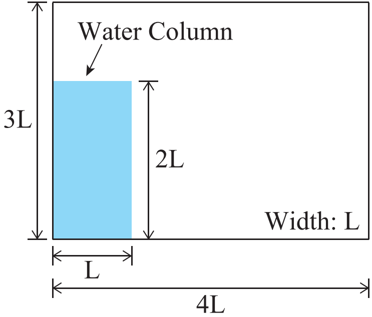

Calculation parameters

Case No.	Mach	Δt (s)	stability
Case 1	0.30	1.06×10^{-4}	unstable
Case 2	0.15	5.28×10^{-4}	stable
Case 3	0.10	3.52×10^{-5}	stable
Case 4	0.010	3.52×10^{-6}	stable
Case 5	0.0010	3.52×10^{-7}	unstable

Figure: Initial setting (left), Calculation parameters (right)

Results: Dimensionless position of the surge front

A validation of the Mach number setting

- Domain settings: Martin & Moyce (1952)

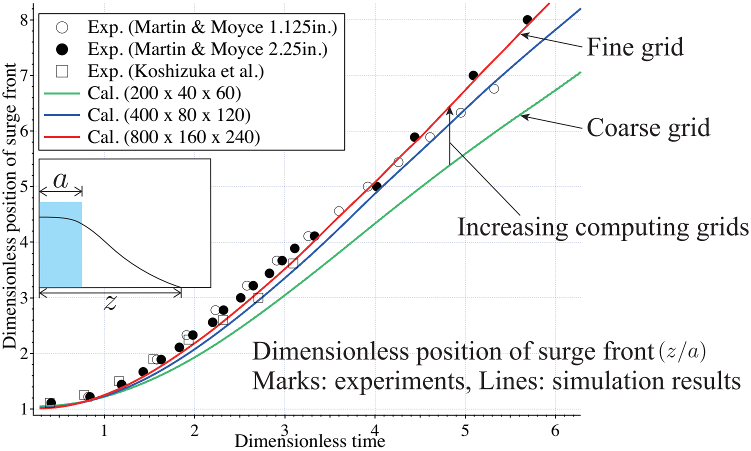

Figure: Timeseries of the dimensionless position of the surge front

V&V: Dam-breaking flows with obstacle (Kölke 2005)

- Classical dam-breaking flows around obstacle
- Validation the accuracy of interface normal and face velocity

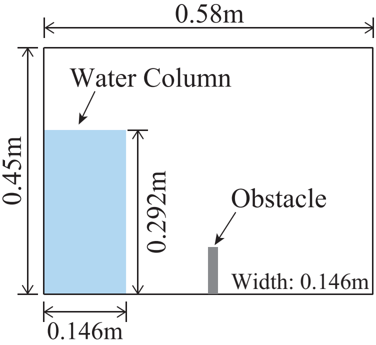

Param.	Value
T_{max}	0.5s
Domain	[0.58 , 0] × [0 , 0.45]
Water	[0.146 , 0] × [0 , 0.292]
Obstacle	[0.015 , 0] × [0 , 0.08]
Grid 1	116 × 29 × 90
Grid 2	232 × 58 × 180
Grid 3	464 × 116 × 360

Figure: Initial setting (left), Calculation parameters (right)

Animation: Three-dimensional view

Results: Interface shapes (two-dimensional view)

- Our model can reproduce the experiment in high resolution
- LBM's boundary condition in "corner grid" must be modified

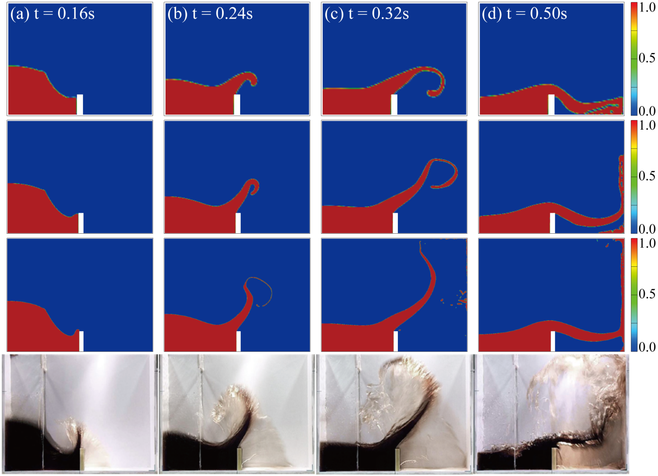

Figure: Grid1, Grid2, Grid3, experimental data, from top to bottom

Verification: Breaking wave (Lubin & Glockner 2003)

- Three-dimensional breaking wave in a rectangular tank
- Verification robustness of our model in such complex flow

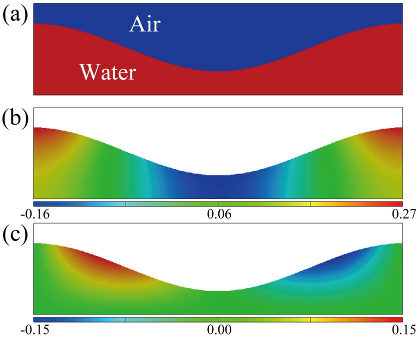

Param.	Value
Grid 1	256 × 32 × 64
Grid 2	512 × 64 × 128
Grid 3	1024 × 128 × 256

(a) Initial total water depth.

(b) Initial horizontal velocity profile.

(c) Initial vertical velocity profile.

Figure: Initial setting (left), Calculation parameters (right)

Animation: Three-dimensional view

Results: Free surface shapes in two-dimensional view

- Our model calculated the breaking wave well
  → A useful tool to simulate tsunami in three-dimension
- The treatment of free surface velocities requires carefully

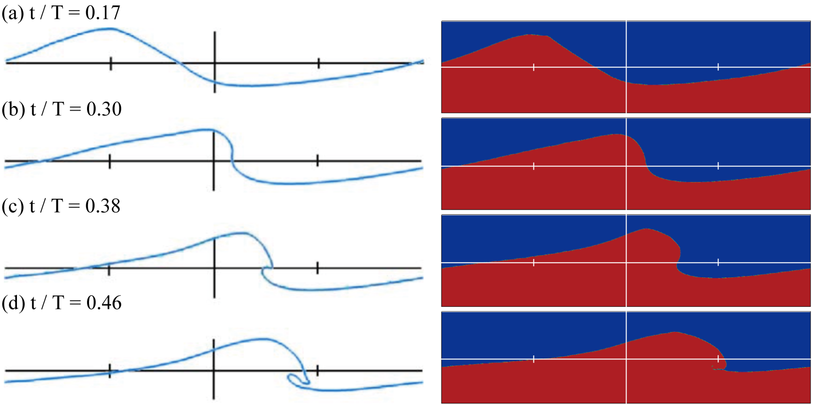

Figure: Lubin & Glockner's results (left), our results (right)

Conclusion and future work

Conclusion

Remarkable features of our free surface model

1. Fully explicit in time integration
2. Seamless free surface shapes
3. Robustness in complex flows (e.g. breaing wave)

Future work

- Model improvement and development
    1. 2D-3D Hybrid tsunami simulation model
    2. Surface tension (additional)
- Further validation (flows around obstacle, etc...)
- Acceleration of codes

Setup LBM: The lattice Boltzmann equation

The lattice Boltzmann equation

$$\underbrace{f_i\left(\boldsymbol{x}+\boldsymbol{e}_i\Delta t, t+\Delta t\right)-f_i\left(\boldsymbol{x}, t\right)}_{\text{Streaming}}=\underbrace{\Omega_i\left[f_i\left(\boldsymbol{x}, t\right)\right]}_{\text{Collision}}$$

The computing algorithms of LBM

1. Streaming: copy the neighboring functions f_i
2. Collision: compute the particles' collision, purely local

Advantages of the lattice Boltzmann equation

1. Fully explicit method: No need to solve the Poisson equation
2. Fully advection scheme: No truncation error in advection term

Setup LBM: Multiple-Relaxation-Time (MRT) model

Key features of the MRT-LBM

- Transforming functions f_i into the independent moments
- Collision the functions by the independent relaxation time

The moment space in D3Q19 lattice model

The definition of moment space $\boldsymbol{m}$ in D3Q19 (Tölke *et al.* 2006)

$$\boldsymbol{m} = (\rho, e, \epsilon, j_x, q_x, j_y, q_y, j_z, q_z, 3p_{xx}, 3\pi_{xx}, p_{ww}, \pi_{ww}, p_{xy}, p_{yz}, p_{zx}, m_x, m_y, m_z)$$

Transforming matrix M always satisfy the following condition:

$$|m\rangle = \mathrm{M}\,|f\rangle\,, \ \ |f\rangle = \mathrm{M}^{-1}\,|m\rangle$$

Collision term of the MRT-LBM

$$\Omega_l\left[f_i\left(\boldsymbol{x}, t\right)\right] = \mathrm{M}^{-1}\mathrm{S}_l\left[\left(\mathrm{M}\boldsymbol{f}\right) - \boldsymbol{m}^{eq}\right]$$

Setup LBM: Multiple-Relaxation-Time (MRT) model

The ket-componets of transforming matrix $\mathbb{M}$

- Creating the matrix from D3Q19 model's vector componets $\boldsymbol{e}_i$
- Two formulations exist in D3Q19 model (return same results) (Tölke *et al.* 2006, d'Humières *et al.* 2002)

$$\Phi_{1,i} = n1, \;\; \Phi_{2,i} = \boldsymbol{e}_i^2 - c^2$$

$$\Phi_{3,i} = 3\left(\boldsymbol{e}_i^2\right)^2 - 6\boldsymbol{e}_i^2 c^2 + c^4$$

$$\Phi_{4,i} = e_{ix}, \;\; \Phi_{6,i} = e_{iy}, \;\; \Phi_{8,i} = e_{iz}$$

$$\Phi_{5,i} = \left(3\boldsymbol{e}_i - 5c^2\right) e_{ix}, \;\; \Phi_{7,i} = \left(3\boldsymbol{e}_i - 5c^2\right) e_{iy}, \;\; \Phi_{9,i} = \left(3\boldsymbol{e}_i - 5c^2\right) e_{iz}$$

$$\Phi_{10,i} = 3e_{ix}^2 - \boldsymbol{e}_i^2, \;\; \Phi_{12,i} = e_{iy}^2 - e_{iz}^2$$

$$\Phi_{14,i} = e_{ix}e_{iy}, \;\; \Phi_{15,i} = e_{iy}e_{iz}, \;\; \Phi_{16,i} = e_{iz}e_{ix}$$

$$\Phi_{11,i} = \left(2\boldsymbol{e}_i^2 - 3c^2\right)\left(3e_{ix}^2 - \boldsymbol{e}_i^2\right), \;\; \Phi_{13,i} = \left(2\boldsymbol{e}_i^2 - 3c^2\right)\left(e_{iy}^2 - e_{iz}^2\right)$$

$$\Phi_{17,i} = \left(e_{iy}^2 - e_{iz}^2\right) e_{ix}, \;\; \Phi_{18,i} = \left(e_{iz}^2 - e_{ix}^2\right) e_{iy}, \;\; \Phi_{19,i} = \left(e_{ix}^2 - e_{iy}^2\right) e_{iz}$$

Setup LBM: Multiple-Relaxation-Time (MRT) model

The equilibrium functions in moment space $\boldsymbol{m}^{eq}$

The functions are determined by density fluid ρ and velocity $\boldsymbol{u}$ as:

$$m_1^{eq} = \rho, \;\; m_4^{eq} = \rho_0 u_x, \;\; m_6^{eq} = \rho_0 u_y, \;\; m_8^{eq} = \rho_0 u_z$$

$$m_2^{eq} = e^{eq} = \rho_0 \left(u_x^2 + u_y^2 + u_z^2 \right)$$

$$m_{10}^{eq} = 3p_{xx}^{eq} = \rho_0 \left(2u_x^2 - u_y^2 - u_z^2 \right)$$

$$m_{12}^{eq} = p_{zz}^{eq} = \rho_0 \left(u_y^2 - u_z^2 \right)$$

$$m_{14}^{eq} = p_{xy}^{eq} = \rho_0 u_x u_y, \;\; m_{15}^{eq} = p_{yz}^{eq} = \rho_0 u_y u_z, \;\; m_{16}^{eq} = p_{zx}^{eq} = \rho_0 u_z u_x$$

where ρ_0 is constant density ($\rho_0 = 1$)

Setup LBM: Multiple-Relaxation-Time (MRT) model

The relaxation matrix in moment space $\mathrm{S}_{l,i}$

The definition of the matrix in D3Q19 model (Tölke *et al.* 2006)

$$s_{l,2,2} = s_{l,a}$$

$$s_{l,3,3} = s_{l,b}$$

$$s_{l,5,5} = s_{l,7,7} = s_{l,9,9} = s_{l,c}$$

$$s_{l,11,11} = s_{l,13,13} = s_{l,d}$$

$$s_{l,10,10} = s_{l,12,12} = s_{l,14,14} = s_{l,15,15} = s_{l,16,16} = -\frac{1}{\tau_l} = s_{l,\omega}$$

$$s_{l,17,17} = s_{l,18,18} = s_{l,19,19} = s_{l,e}$$

Relaxation parameters of conserved macro-scopic values

- Density and momentum are conserved in athermal fluid
- Non-conserved values approach the equilibrium (stable state)

The relaxation matrix except for $s_{l,\omega}$ can be determined as:

$$s_a = s_b = s_c = s_d = s_e = -1.0$$

Overview: The pseudo-compressibility of LBM

The non-dimensional values of Mach number

Mach number Ma satisfies the following formula using Knudsen number Kn and Reynolds number Re:

$$\mathrm{Ma} \sim \mathrm{Kn} \cdot \mathrm{Re}$$

When Re has a finite limit and Kn approaches 1,
Chapman-Enskog expansion can be used by parameter $\epsilon = O\left(\Delta x\right)$

The Chapman-Enskog expansion

A perturbation expansion of the velocity distribution functions f_i under low Mach condition

$$f_i = f_i^{(0)} + \epsilon f_i^{(1)} + \epsilon^2 f_i^{(2)} + \epsilon^3 f_i^{(3)} + \epsilon^4 f_i^{(4)} \cdots$$

Macro-scopic equations (Navier-Stokes equations) can be obtained by the Taylor expansion of the lattice Boltzmann equation

Overview: The pseudo-compressibility of LBM

The sound speed and Mach number

General definition:

$$\mathrm{Ma} \sim \frac{\|u_{\max}\|}{c_s}$$

where $\|u_{\max}\|$ is the maximum velocity in flow field

The macro-scopic equations (He & Luo 1997)

Results of the Chapman-Enskog expansion:

$$\nabla \cdot \boldsymbol{u} = 0 + O\left(\mathrm{Ma}^2\right)$$

$$\frac{\partial \boldsymbol{u}}{\partial t} + \boldsymbol{u} \cdot \nabla \boldsymbol{u} = -\nabla p + \nu \nabla^2 \boldsymbol{u} + O\left(\mathrm{Ma}^3\right)$$

Key features of LBM's simulation

1. The pseudo-compressibility appears in $O\left(\mathrm{Ma}^2\right)$
2. $\mathrm{Ma} < 0.15$ for incompressible flows

Overview: The pseudo-compressibility of LBM

The definition of the sound speed in LBM

The sound speed c_s in LBM is defined by Δx and Δt as:

$$c_s = \frac{e}{\sqrt{3}} = \frac{\Delta x}{\sqrt{3}\Delta t}$$

→ The pseudo-compressibility must be controlled by time step Δt

The maximum velocity in dam-breaing flows (Stansby 1998)

Analogically based on the shallow water theory:

$$\|u_{\max}\| = 2\sqrt{gH}$$

where g is the gravity acceralation and H is the initial water height

Algorithm: Interface normal (Pillod & Puckett 2007)

The most accurate method in explicit approach

$$\nabla C = \frac{1}{2\Delta x} \left(\begin{array}{l} \bar{C}_x\left(\boldsymbol{x}+1\right) - \bar{C}_x\left(\boldsymbol{x}-1\right) \\ \bar{C}_y\left(\boldsymbol{x}+1\right) - \bar{C}_y\left(\boldsymbol{x}-1\right) \\ \bar{C}_z\left(\boldsymbol{x}+1\right) - \bar{C}_z\left(\boldsymbol{x}-1\right) \end{array} \right)$$

where $\bar{C}$ is the averaged fluid fraction defined as follows:

$$\bar{C}_x\left(x,y,z\right) = \sum_{i=-1}^{1}\sum_{j=-1}^{1} C\left(x, y+i, z+j\right) \cdot w_{i,j}$$

$$\bar{C}_y\left(x,y,z\right) = \sum_{i=-1}^{1}\sum_{j=-1}^{1} C\left(x+i, y, z+j\right) \cdot w_{i,j}$$

$$\bar{C}_z\left(x,y,z\right) = \sum_{i=-1}^{1}\sum_{j=-1}^{1} C\left(x+i, y+j, z\right) \cdot w_{i,j}$$

$w_{i,j}$ is the weighting function in Pillod & Puckett (2007)

Algorithm: Determination of distance parameter

A root finding in PLIC-VOF (Scardovelli & Zaleski 2000)

Parameter α is estimated by the inverse problem of reconstruction (i.e. The fluid fraction is given as the area $ABNKHGML$)

$$C = \frac{1}{6n_1n_2n_3}\left[\alpha^3 - \sum_{i=1}^{3} F_3\left(\alpha - n_i\Delta x\right) + \sum_{i=1}^{3} F_3\left(\alpha - \alpha_{\max} + n_i\Delta x\right)\right]$$

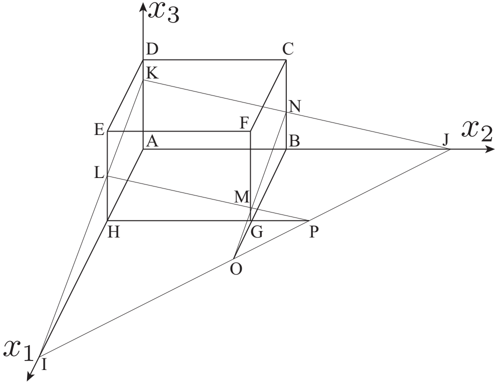

Algorithm: Evaluation of the fluid flux

Lagrangian-Explicit method (Aulisa *et al.* 2007)

The line segments move toward neighboring cells directly
(i.e. α and $\boldsymbol{n}$ are updated by face velocity in the next time step)

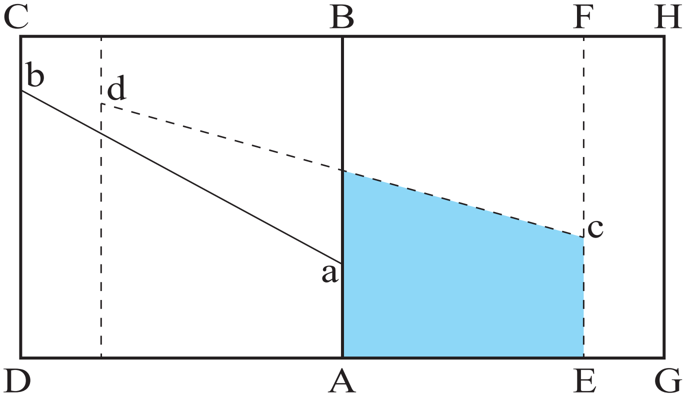

Figure: The interface advection by the Lagrangian-Explicit approach

Algorithm: Time evolution of the fluid fraction

The fluid fraction at the next time step

Lagrangian-Explicit method directly exchanges macro-scopic flux
The fraction level at the next time step C^{t+1} can be calculated as:

$$C^{t+1} = VL_{i+1,j} + VC_{i,j} + VR_{i-1,j}$$

The split method is used for multiple-dimension advection

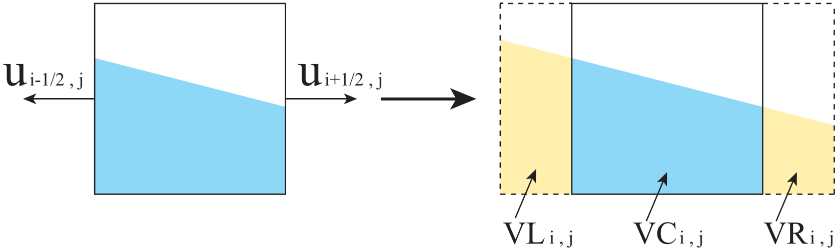

Figure: The mass exchange between neighboring cells by the PLIC-VOF

Verification: Lid-driven cavity flows (Ku *et al.* 1987)

A code verification of the MRT-LBM without free surface

- A primitive verification of the MRT-LBM
- Up to steady states (without turbulence model)

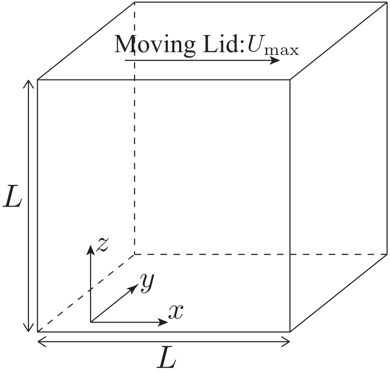

Calculation parameters

Parameter	Value
Resolution	$128\times128\times128$
L	1.0
$U_{\max}$	0.1
Re	100, 400, 1000

Relaxation rate is given as:

$$\tau = 3\frac{U_{\max}L}{\mathrm{Re}} + \frac{1}{2}$$

Figure: Initial setting (left), Calculation parameters (right)

Results: Spacing velocity profiles

A comparison between the MRT-LBM and Ku *et al.* (1987)

- Spacing velocity profiles in steady state $(\mathrm{Re} = 1000)$
- Our calculation code are in good agreement with Ku *et al.* simulation results

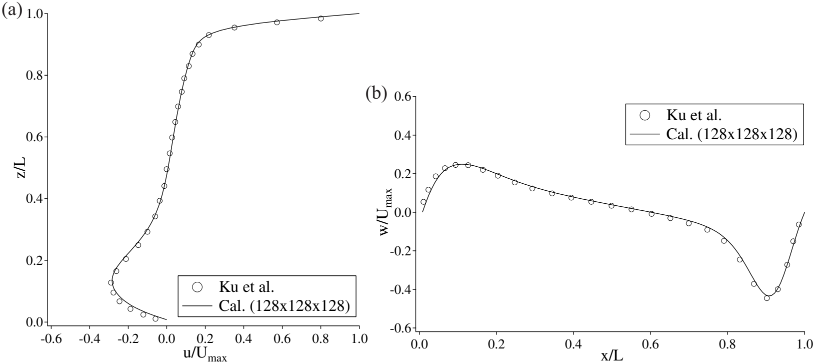

Figure: Spacing velocity profiles, x-axis (left), z-axis (right)

Verification: Non-linear standing wave (Wu & Taylor 1994)

A numerical investigation of the pseudo-compressibility

- A Comparison verification of the MRT-LBM and BGK-LBM
- Total simulation time: $5.0\mathrm{s}$
- Spacing resolution: $(x, y, z) = (400 \times 100 \times 300)$

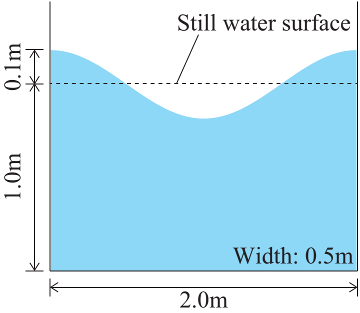

Calculation parameters

Case No.	Mach	Δt (s)	stability
Case 1	0.30	2.77×10^{-4}	unstable
Case 2	0.15	1.38×10^{-4}	stable
Case 3	0.10	9.22×10^{-5}	stable
Case 4	0.010	9.22×10^{-6}	stable
Case 5	0.0010	9.22×10^{-7}	unstable

Figure: Initial setting (left), Calculation parameters (right)

Animation: Three-dimensional view

Results: Spacing density profiles

- Both collision models satisfy the incompressible condition
- MRT-LBM: Natural profiles
- BGK-LBM: Non-physical, numerical oscillation

MRT is needed to simulate free surface flows by LBM approaches

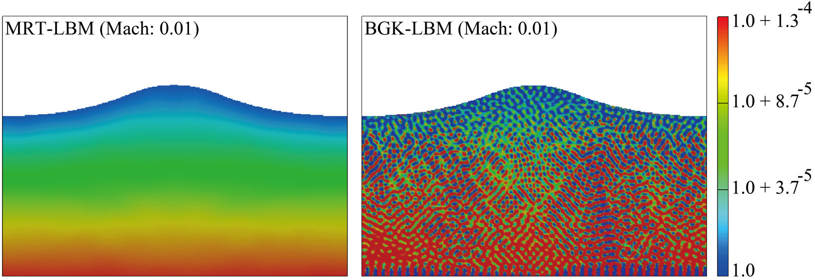

Figure: Fluid density profiles of the BGK-LBM and MRT-LBM at $t = 0.5\mathrm{s}$

Results: Timeseries of the water level

- Linear theory: The linear solution of the Stokes' theory
- Second order theory: The second order solution (non-linear)

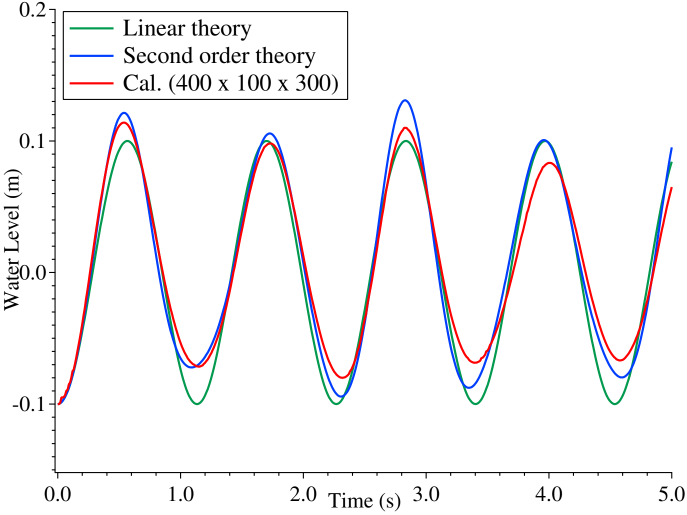

Figure: Timeseries water level at the center of the numerical tank